

Hysteretic transition between avalanches and continuous flow in rotated granular systems

Stefan J. Linz, Wolfgang Hager, and Peter Hänggi

Theoretische Physik I, Institut für Physik, Universität Augsburg, D-86135 Augsburg, Germany

(Received 16 December 1998; accepted for publication 4 May 1999)

Experiments in drums or cylinders partly filled with a granular system and rotated constantly about their horizontally aligned axis of symmetry show a hysteretic transition from discrete avalanches to continuous flow if the rotation rate is adiabatically changed. Herein, we show that this hysteresis can be explained by the impact of global Langevin-type fluctuations in a recently proposed minimal model for surface flow along granular piles. For too large magnitudes of the fluctuations corresponding to almost elastic grains, the hysteresis vanishes. This might explain why molecular dynamical simulations were not yet able to detect the hysteretic transition. © 1999 American Institute of Physics. [S1054-1500(99)01203-3]

Granular surface flow along granular piles in rotated drums shows, for small rotation rates, an interesting hysteretic transition between stick–slip dynamics and continuous flow. Experimentally, this transition is generically hysteretic. In molecular dynamical simulations of the microdynamics of these large assemblies of grains, however, this type of transition has not been seen so far. We present a simple stochastic dynamical model that combines the basic macromechanical mechanisms of granular surface flow and detect the experimentally observed type of hysteretic transition for small, but nonzero fluctuation strength. For larger fluctuation strength, the hysteretic behavior disappears. This might resolve the aforementioned discrepancy between experimental and molecular dynamical findings.

I. BASICS

Since the late 1980s, there has been a steadily increasing fascination with particulate or granular systems observable in the physics community.¹ It stems from the poor understanding of the dissipative dynamics of these large assemblies of extended massive particles of complicated shape which interact only repulsively through inelastic collisions and friction. The interplay between the complexity of the micromechanics of this classical many-particle system and its comparably simple (although often surprising) dynamics on a macroscopic level is the major challenge in this field. Lacking yet any theoretically manageable *ab initio* theory for the dynamics of granular systems, physicists are mainly discussing specific paradigmatic setups that (i) can be investigated experimentally and numerically, e.g., by using molecular dynamical simulations, (ii) allow theoretical modeling and therefore, (iii) lead to insights in the governing physical mechanisms. Among others,¹ the dynamics of avalanches and surface flow in rotated drums or cylinders plays a very prominent role in detecting generic features of granular dynamics.

The piling of granular systems in partly filled drums

shows most clearly the non-Newtonian fluid behavior of particulate matter. Up to an inclination angle φ_s of the surface of the granular pile, the system stays at rest; increasing the inclination angle φ beyond the *maximum angle of repose* φ_s , the upper grain layers of the pile start to slip, and the inclination angle decreases until the avalanche stops at the minimum angle of repose φ_r . As pioneered by Jaeger *et al.*² and Rajchenbach,³ rotation of the drum about its horizontally aligned axis of symmetry with a constant rotation rate $\bar{\omega}$ leads to two very distinct types of dynamics of the surface flow. For small $\bar{\omega}$, one observes almost periodic stick–slip dynamics (SSD) alternating between avalanches and rigid pile rotations. For larger $\bar{\omega}$, the pile exhibits a continuous surface flow dynamics (CFD) with an almost constant inclination angle φ_{CFD} being proportional to $\bar{\omega}^2$.

A specific, but nevertheless important problem in this context is the nature of the transition from SSD to CFD. As found in the experiment of Rajchenbach,³ this transition is *hysteretic*: The transition from SSD to CFD while adiabatically *increasing* $\bar{\omega}$ occurs at a threshold value $\bar{\omega}_T^{(1)}$, whereas the transition value from CFD to SSD while adiabatically *decreasing* $\bar{\omega}$ happens at $\bar{\omega}_T^{(2)}$, being nonzero and considerably smaller than $\bar{\omega}_T^{(1)}$. The hysteretic character of the transition between SSD and CFD has also been confirmed in other experiments, e.g., Ref. 4, but interestingly, it has not yet been reported in molecular dynamical simulations of rotated granular materials. In particular, Buchholtz *et al.*⁵ explicitly state that they were not able to reproduce the hysteretic character of the transition between SSD and CFD in their simulations; within their numerical resolution, the transition seems to be nonhysteretic. Also the simulations of Dury *et al.*⁶ seem to suggest that the transition from SSD to CFD and vice versa is nonhysteretic for their particular choice of parameter values.

The aim of our paper is to try to resolve this apparent discrepancy by investigating the transition from SSD to CFD in a stochastic extension of a recently proposed deterministic minimal model^{7,8} which explains phenomenologically many

basic properties of the ensemble-averaged avalanche dynamics. Using extensive stochastic simulations, we find that small velocity fluctuations as they occur naturally in particulate systems, can lead to the hysteretic transition as seen in the experiments^{3,4} as well as to a nonhysteretic transition depending on the size of the fluctuations. Our investigation also sheds light on the fundamental interplay between deterministic macroscopic frictional dynamics of granular systems and its superimposed small micromechanically generated stochastics.

II. MACROMECHANICAL MODEL

The basis of our investigation is a model for granular surface flow that extends the previously reported deterministic minimal model (DMM)⁷⁻⁹ for surface flow along granular piles by the incorporation of small stochastic forces. This stochastically extended minimal model recently has been successfully used^{9,10} to understand and explain the spectral statistics of avalanches as seen in the seminal experiments by Jaeger *et al.*² Within this macromechanical modeling approach, the dynamics of the global inclination angle $\varphi(t)$ of the granular pile and the characteristic velocity $v(t)$ of the surface flow (being proportional to the square root of the total kinetic energy of the flow or the moving grains) is represented by the stochastic dynamical system

$$\dot{v} = g[\sin \varphi - (b_0 + b_2 v^2) \cos \varphi + \tilde{\zeta}(t)] \chi(\varphi, v), \quad (1)$$

$$\dot{\varphi} = -a v + \bar{\omega}, \quad (2)$$

with the indicator function for surface flow given by

$$\chi(\varphi, v) = \Theta(v) + \Theta(\varphi - \varphi_s) - \Theta(v) \Theta(\varphi - \varphi_s). \quad (3)$$

Here, $\Theta(y)$ denotes Heaviside's step function [$\Theta(y) = 0$ ($y \leq 0$) ($y > 0$)], a , b_0 , and b_2 are positive constants, g is the gravitational acceleration, and $\bar{\omega}$ the external rotation rate of the drum.

Equations (1) and (2) combine Coulomb's theory of frictional motion on an inclined plane with viscoplastic arguments and the dynamical nature of the surface motion granular systems: (i) a nonlinear dynamic friction coefficient $k_d(v) = b_0 + b_2 v^2$ with $b_0 > 0$ and $b_2 > 0$ in (1) which interpolates between solid and Bagnold friction^{7,8} and is monotonically increasing with v and, therefore, velocity strengthening, (ii) the fact that a granular pile is statically stable until the inclination angle φ_s exceeds the maximum angle of repose, (iii) the fact that a surface flow $v(t)$ is always directed down the pile, $v(t) > 0$, and stops if $v(t)$ reaches zero, and (iv) the fact that a surface flow $v(t) \neq 0$ also excites dynamical changes of the inclination angle φ which counteract the acceleration of the surface flow. Facts (ii) and (iii) are mimicked by the indicator function for flow, χ , given in Eq. (3).

Stochasticity that reflects micromechanically generated, but also macromechanically observable, fluctuations of the inclination angle φ and the global velocity $v(t)$,⁴ enters in the model (1) and (2) through the simplest possible stochastic process, namely by a macromechanical Langevin "force" $\tilde{\zeta}(t)$ being Gaussian white noise with zero mean and a correlation or fluctuation strength given by

$$\langle \tilde{\zeta}(t) \tilde{\zeta}(t') \rangle = \tilde{\Delta}^2 \delta(t - t'). \quad (4)$$

Two remarks are important. (i) The fluctuating "force" is only present when there is flow, $v \neq 0$. It does not act during the rigid pile rotation. (ii) Due to the cross coupling of Eqs. (1) and (2), small "force" fluctuations excite velocity fluctuations as well as fluctuations of the inclination angle of the pile. Both facts are also in accordance with the experiments by Caponeri *et al.*⁴

Although a micromechanical derivation of the Langevin term in Eq. (1) is far beyond the scope of the paper, a micromechanical argument for its presence goes as follows. Inelastic and in general noncentral collisions of grains lead to scattering of the grains, the inhomogeneous bulk network to spontaneous trapping of individual grains and locking of local, small scale avalanches, and the external increase of the inclination angle of the pile to reexcitation of grain motion. Altogether, this creates on the microdynamical scale permanent jerky-like variations of the local kinetic energy. Although these fluctuations are local, also global kinetic energy and, with it, the characteristic velocity $v(t)$ of the surface flow considered as spatial average over the grains in motion, also fluctuates due to the finite extension of the pile. The magnitude of the fluctuations should be directly related to the degree of inelasticity of the grains. Almost inelastic (almost elastic) grains lead to small (large) fluctuations. The existence of small erratic global variations that superimpose the global surface flow dynamics, also have been nicely demonstrated in the experiments by Caponeri *et al.*⁴ and can also be seen in molecular dynamical simulations, see, e.g., Refs. 6 and 11.

Further simplification can be obtained by taking advantage of the experimental observation²⁻⁴ that the angular variations during avalanching are typically small in comparison to the inclination angle of the pile. Basically, the angular dynamics of the avalanches of Eqs. (1) and (2) is centered about the angle $\varphi_d = \tan b_0$.⁷ Introducing the deviation from this angle,

$$\Phi(t) = \varphi(t) - \varphi_d, \quad (5)$$

nondimensionalizing time by $t \rightarrow t/\sqrt{ga}$ and velocity by $v \rightarrow v\sqrt{g/a}$, setting $\omega = \bar{\omega}/\sqrt{ga}$, and performing a small angle approximation in Φ (since the difference $\varphi_s - \varphi_r$ is only a few angular degrees), we obtain the following simplified macromechanical model;

$$\dot{v} = [-\delta v^2 + \Omega_0^2 \Phi + \zeta(t)] \chi(\Phi, v), \quad (6)$$

$$\dot{\Phi} = -v + \omega, \quad (7)$$

where the indicator function for flow is given by

$$\chi(\Phi, \dot{\Phi}) = \Theta(-\dot{\Phi} + \omega) + \Theta(\Phi - \Phi_s) - \Theta(-\dot{\Phi} + \omega) \Theta(\Phi - \Phi_s), \quad (8)$$

and $\Phi_s = \varphi_s - \varphi_d$, $\delta = (gb_2/a) \cos \varphi_d > 0$, and $\Omega_0^2 = 1/\cos \varphi_d > 0$. After nondimensionalization, the fluctuation strength of the stochastic variable $\zeta(t)$ reads $\Delta = \tilde{\Delta}/g$.

In the deterministic limit, $\Delta = 0$, and for small rotation rates ω , the model shows periodic global avalanches which

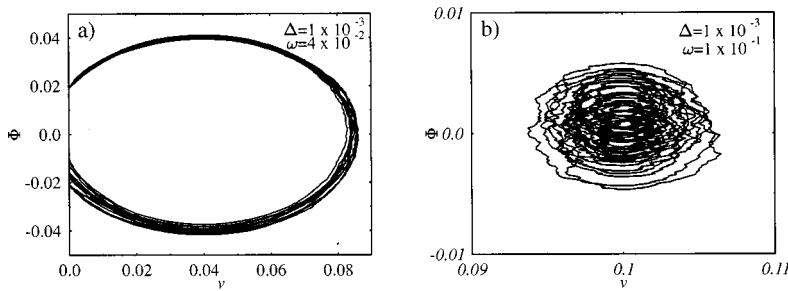


FIG. 1. Representative examples of the effect of the Langevin “forces” on (a) SSD ($\omega=4\times 10^{-2}$) and (b) CFD ($\omega=10^{-1}$) in the (v, Φ) phase space. Parameter values are $\Phi_s=0.0194$, $\delta=0.1$, $\Omega_0=1.1$, and $\Delta=10^{-3}$.

start from $\Phi_s = \varphi_s - \varphi_d$ with $v=0$ and decay to $\Phi_r = \varphi_r - \varphi_d \approx -\Phi_s$ when $v=0$ has been reached again. They are separated by rigid pile rotations until Φ_s is reached again by virtue of the external rotation ω . The duration of the rigid pile rotation is determined by $(\Phi_s - \Phi_r)/\omega$. For larger rotation rates, however, there is a transition to a continuous surface flow with a constant velocity $v_{CFD} = \omega$ and a constant inclination angle $\Phi_{CFD} = \delta\omega^2/\Omega^2$. Note that (i) the existence of this fixed point of Eqs. (6) and (7) is a direct consequence of the dependence of the dynamic friction coefficient on the square of the velocity and (ii) that this result agrees with Rajchenbach’s experimental findings of the dependence of the averaged inclination angle on the rotation rate.

For small enough fluctuation strengths Δ , this basic mechanism is still present in the stochastically extended model, Eqs. (6) and (7), however, with superimposed small stochastic variations of the velocity of the surface flow and the inclination angle of the pile.

III. RESULTS

In this section, we present the results of extensive numerical simulations of the macromechanical model, Eqs. (6) and (7), that show the drastic impact of Langevin forces on the transition between SSD and CFD for the granular surface flow. The parameter values, $\Phi_s=0.0194$, $\delta=0.1$, and $\Omega_0=1.1$, we use in these simulations of the model, Eqs. (6) and (7), are extrapolations from experimental data in Refs. 3 and 4. For further details we refer to Refs. 7, 8, and 10.

A. Perturbed SSD and CFD states

For small correlation strength Δ , the main effects of the stochastic forces on the dynamics are as follows. (a) In the stick–slip regime corresponding to small ω , the duration of the avalanches is no longer constant, but is distributed about the average avalanche duration $\langle T_{av} \rangle$, which is practically given by its deterministic limit. As our numerical calculations show, this distribution is roughly Gaussian. Another effect is that the duration of the rigid-pile-rotation T_{rpr} is also a stochastically distributed quantity, even though the next avalanche again starts sharply at the maximum angle of repose φ_s . (b) In the continuous flow range corresponding to larger ω , the velocity of the continuous surface flow and the inclination angle of the pile do not reach a steady state, but fluctuate about their mean values. For the small fluctuation strengths considered here, the mean values are basically equal to the deterministic fixed point mentioned above. To substantiate that stochastically perturbed SSD and CFD dynamics can still be distinguished, we show as representative

examples in Fig. 1 the dynamics of the perturbed SSD and CFD states in the phase space spanned by v and Φ . Note that in the presence of external rotation the maximum and minimum angles of inclination of the pile for SSD occur during the avalanching process in the form of an inertia-related over- and undershooting effect. This effect has also been reported in the experiments in Ref. 4.

B. Definition of SSD and CFD and order parameters

For nonzero fluctuation strength Δ and very close to the transition point from SSD to CFD and vice versa, one finds numerically that the dynamics of the surface flow in the model (6) switches erratically between avalanching and continuous flow. In order to distinguish between SSD and CFD states in our simulations of the surface flow dynamics, one has to define more precisely a SSD and CFD state. As a convenient criterion for our simulations, a large fixed number N of successive avalanches without any jump to CFD has been used to characterize a SSD state. If during the simulations such long sequences of avalanches could not be observed, it has been identified as a CFD state. In our simulations, we used $N=200$.

To analyze and quantify the transitions from discrete avalanches to continuous flow and vice versa, it is necessary to introduce the appropriate order parameters which (i) allow a clear distinction between both dynamics and (ii) are accessible from the experimental point of view. At first sight, one might expect that the time average of the reduced inclination angle, $\langle \Phi \rangle$, already presents such a quantity that is sensitive enough for such a distinction. As our simulations showed, however, there are hardly any changes in $\langle \Phi \rangle$ observable if the dynamics of the surface flow switches from SSD to CFD. For demonstration purposes, we use in the SSD range the time average of the maximum and minimum angle of inclination $\langle \Phi_{max} \rangle$ and $\langle \Phi_{min} \rangle$ occurring during avalanching, whereas in the CFD range the averaged inclination angle $\langle \Phi_{CFD} \rangle$ is used.

C. Adiabatic increase and decrease of the rotation rate

In this section, we show that the incorporation of stochasticity can lead to the type of hysteretic transition as seen in the experiments.^{3,4} We consider two cases: the deterministic case, $\Delta=0$, and the stochastic case with a fluctuation strength $\Delta=8\times 10^{-4}$. In both cases, we investigate the transition from SSD to CFD and back to SSD again in the model, Eqs. (6) and (7), by (i) *adiabatically increasing* the rotation rate ω

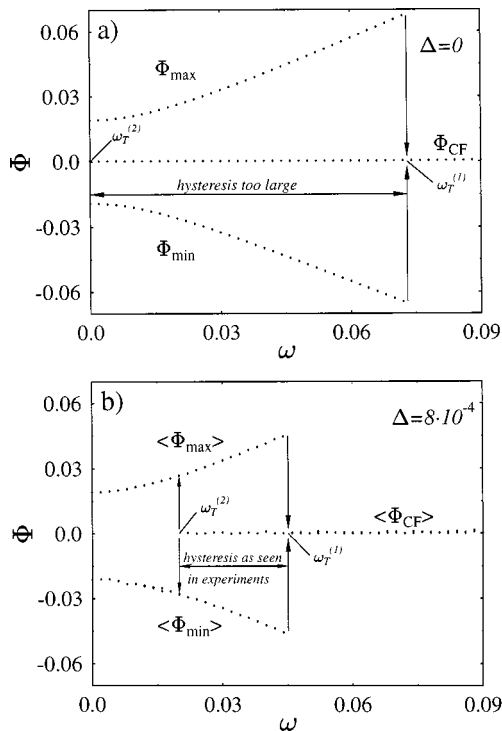


FIG. 2. Hysteretic transition between SSD and CFD for (a) $\Delta=0$ and (b) $\Delta=8 \times 10^{-4}$. In the SSD state, the maximum (minimum) angles during flow are $\langle \Phi_{\max} \rangle$ ($\langle \Phi_{\min} \rangle$). At $\omega_T^{(1)}$ the transition from SSD to CFD occurs, and at $\omega_T^{(2)}$ the transition from CFD to SSD.

until a CFD state has been reached and then (ii) subsequently decreasing the rotation rate ω in an adiabatic way again. By doing that, we are able to detect the two transition points $\omega_T^{(1)}$ from SSD to CFD and $\omega_T^{(2)}$ from CFD back to SSD. The result for the zero and the representative nonzero fluctuation strength Δ is shown in Fig. 2.

In Fig. 2(a), the deterministic limit of model (6) and (7) ($\Delta=0$) is depicted. Increasing ω from zero, the broadening of the SSD limit cycle in the phase space spanned by v and Φ can be seen. This is reflected by the increase of the modulus of maximum and minimum angle of inclination Φ_{\max} and Φ_{\min} , respectively, that occur during avalanching due to the aforementioned over- and undershooting effect. The sudden transition from SSD to CFD at $\omega_T^{(1)} \approx 0.074$ occurs if $\Phi=0$ and $v=0$ are reached simultaneously. Decreasing ω again, the surface flow dynamics is caught in the CFD fixed point which is linearly stable against small perturbations as they occur when the rotation rate is lowered. Due to the lack of a destabilization mechanism for the continuous flow, however, the system remains in the CFD solution until $\omega_T^{(2)}=0$, when ω is adiabatically decreased. As a consequence, the deterministic limit of the granular surface flow model exhibits hysteresis. It is, however, too large in comparison to the experimental findings^{3,4} where $\omega_T^{(2)}$ is nonzero.

In Fig. 2(b), the dynamics of the stochastically extended model (6) and (7) is depicted. For small enough rotation rates the averaged broadening of the perturbed SSD limit cycle in the phase space spanned by v and Φ is quantitatively the same as in the deterministic limit. However, the transition from SSD to CFD represented by the jumps from $\langle \Phi_{\max} \rangle$ and

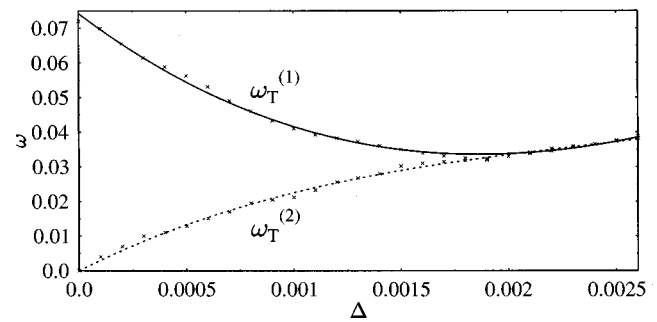


FIG. 3. The dependence of the transition points $\omega_T^{(1)}$ and $\omega_T^{(2)}$ on the fluctuation strength Δ . The model parameters are $\Phi_s=0.0194$, $\delta=0.1$, and $\Omega_0=1.1$.

$\langle \Phi_{\min} \rangle$ to $\langle \Phi_{\text{CFD}} \rangle$ is largely reduced and happens at $\omega_T^{(1)} \approx 0.045$. Above that value, the surface flow is in the CFD state. Lowering the rotation rate again leads to the *major effect* of the Langevin term in Eq. (6). The transition from CFD to SSD at $\omega_T^{(2)}$ represented by the jumps from $\langle \Phi_{\text{CFD}} \rangle$ to $\langle \Phi_{\max} \rangle$ and $\langle \Phi_{\min} \rangle$ occurs at a *nonzero* value of ω . The value of the fluctuation strength $\Delta=8 \times 10^{-4}$ has been chosen such that there is a striking agreement with the experimental findings of Rajchenbach.³ There, the transition from CFD to SSD, $\omega_T^{(2)}$, occurs at a rotation rate that is slightly smaller than half of the rotation rate for the transition from SSD to CFD, $\omega_T^{(1)}$.

D. Fluctuation strength dependence of the hysteresis

In this section, we numerically investigate the location of the transition points from SSD to CFD, $\omega_T^{(1)}$, and from CFD to SSD, $\omega_T^{(2)}$, as a function of the fluctuation strength Δ . The results are shown in Fig. 3. The crosses in Fig. 3 denote the numerically obtained data of the stochastic simulations. The solid and the dotted lines represent smooth interpolations of the data for $\omega_T^{(1)}$ and $\omega_T^{(2)}$, respectively. For the deterministic case, $\Delta=0$, one recovers the analytically known result that $\omega_T^{(1)} \approx 0.074$ and $\omega_T^{(2)}=0$. Increasing Δ from zero has three major effects.

First, the transition points $\omega_T^{(1)}$ from SSD to CFD (the upper curve in Fig. 3) decrease with increasing, but still small enough Δ until a minimum of $\omega_T^{(1)}$ at about $\Delta=0.002$ is reached. The decrease $\omega_T^{(1)}$ with Δ results from the fact that for nonzero Δ the minimum angle of repose Φ_r is distributed about its mean $\langle \Phi_r \rangle$. The latter is basically determined by its deterministic value. Since the width of this distribution increases with Δ , the dynamics can escape to the CFD dynamics for smaller rotation rates than in the deterministic case. For larger Δ , $\omega_T^{(1)}$ slightly increases again.

Second, the transition points $\omega_T^{(2)}$ from CFD to SSD (the lower curve in Fig. 3) are nonzero as soon as Δ is nonzero and they increase, at least for larger Δ , weaker than linear with increasing fluctuation strength. At least for very small Δ this can be explained as follows. Since the velocity $v(t)$ of CFD fluctuates about its mean, it can reach $v=0$ for nonzero ω . After reaching $v=0$, the system is trapped in the SSD state. Since the width of the v distribution is proportional to Δ , one must expect a linear increase of $\omega_T^{(2)}$ for small Δ .

Third, the curves for $\omega_T^{(1)}$ and $\omega_T^{(2)}$ approach each other and apparently merge above $\Delta \approx 0.002$. Within our numerical resolution, the difference between both curves cannot be distinguished above $\Delta \approx 0.0021$.

What are the consequences for the dynamics in a rotated drum experiment? Below $\omega_T^{(2)}$ only SSD exists, whereas above $\omega_T^{(1)}$, only CFD can exist. The wedge-shaped area enclosed by $\omega_T^{(1)}$ and $\omega_T^{(2)}$ in Fig. 3 represents the combinations of rotation rates ω and fluctuation strengths Δ , where hysteresis, i.e., a coexistence of SSD and CFD states, occurs. The hysteretic range bounded by $\omega_T^{(1)}$ and $\omega_T^{(2)}$ shrinks with increasing fluctuation strength Δ until merging occurs. Moreover, for larger fluctuation strengths Δ beyond the merging, the transition from SSD to CFD is nonhysteretic and increases with increasing Δ .

We note that the transition curves $\omega_T^{(1)}$ and $\omega_T^{(2)}$ have some dependence on the definition of the stochastically perturbed SSD and CFD states. As mentioned above, we used $N=200$ successive avalanches for a SSD state. For a smaller number of avalanches entering in the criterion, the merging point of $\omega_T^{(1)}$ and $\omega_T^{(2)}$ is shifted to slightly larger Δ . The scenario depicted in Fig. 3, however, remains qualitatively unchanged under a modification of N .

So far, the fluctuation strength Δ is a parameter in the model. As we have argued above, the degree of inelasticity of the grains might be the key to understanding the magnitude of the fluctuations entering in the stochastic model. It is likely that the fluctuation strength for systems with comparably weak inelastic or, equivalently, almost elastic grains as used in the micromechanical simulations is so large that the corresponding fluctuation strength Δ lies outside the hysteretic area in Fig. 3. On the other hand, more inelastic grains as they are used in the experiments^{3,4} seem to correspond to a fluctuation strength Δ that lies inside the hysteretic area in Fig. 3. If our scenario is correct it implies that there is no real discrepancy between experimental results and molecular dynamical simulations. It is just the question of the strength of the macromechanical fluctuations and, therefore, the microstructure of the grains that matters.

IV. SUMMARY AND DISCUSSION

We have shown that the hysteretic transition from discrete avalanches to continuous flow in rotated drums as found in experiments 3 and 4 can be understood as a transition being induced by the impact of small Langevin ‘‘forces’’ in the deterministic minimal model for granular surface flow.^{7,8} This stochastically extended minimal model also offers a possible explanation why this hysteretic transition has not yet been seen in molecular dynamical simula-

tions of granular drum flow. Hysteresis can only occur as long as the fluctuation strength Δ is below some limit. For larger fluctuation strength, the transition from SSD to CFD is nonhysteretic. The magnitude of the fluctuations is clearly related to micromechanical properties of the granular system such as, e.g., the degree of inelasticity of the grains. The reason why the hysteretic transition has not yet been observed in molecular dynamical simulations might be caused by too weak inelasticity of the grains in comparison to the experiments.^{3,4}

We also note that our approach seems to be distinct from previous proposals^{4,12,13} that explained the hysteretic transition on a deterministic level by introducing a negative differential minimum in the dynamical friction coefficient. In our approach, it is the stochasticity of the surface flow dynamics that is responsible for the transition of CFD to SSD occurring at a *nonzero* rotation rate $\omega_T^{(2)}$. It remains an open problem for future investigations which of the two macromechanical explanations is the most adequate one for granular surface flow. We hope that our investigation stimulates sensitive experiments and *ab initio* micromechanical simulations in order to test our predictions.

ACKNOWLEDGMENTS

The authors acknowledge support by the *Graduiertenkolleg: Nichtlineare Probleme in Analysis, Geometrie und Physik* (GRK 283) financed by the Deutsche Forschungsgemeinschaft and the state of Bavaria.

¹For an overview see: H. M. Jaeger, S. R. Nagel, and R. P. Behringer, *Rev. Mod. Phys.* **68**, 1259 (1996); *Science* **255**, 1523 (1992); H. M. Jaeger *et al.*, *MRS Bull.* **XIX**, 25 (1994).

²H. M. Jaeger, C.-H. Liu, and S. Nagel, *Phys. Rev. Lett.* **62**, 1988 (1989).

³J. Rajchenbach, *Phys. Rev. Lett.* **65**, 2221 (1990).

⁴M. Caponeri, S. Douady, S. Fauve, and C. Larouche, NSF Report No. NSF-ITP-92-140 (1992) (unpublished); S. Fauve (private communication).

⁵V. Buchholtz, T. Pöschel, H.-J. Tillemans, *Physica A* **216**, 199 (1995).

⁶C. Dury and G. Ristow (unpublished); C. M. Dury, G. H. Ristow, and M. Nakagawa, ‘‘Angle of Repose in a Rotating Drum,’’ in *Powders & Grains, Vol. 97*, edited by R. P. Behringer and J. T. Jenkins (Balkema, Rotterdam, 1997), p. 507; G. Ristow, Habilitation thesis, Universität Marburg, 1998.

⁷S. J. Linz and P. Hänggi, *Phys. Rev. E* **51**, 2538 (1995).

⁸S. J. Linz and P. Hänggi, *Phys. Rev. E* **50**, 3464 (1994); *Physica D* **97**, 577 (1996); S. J. Linz, *Lect. Notes Phys.* **484**, 306 (1997).

⁹S. J. Linz, Habilitation thesis, Universität Augsburg, 1997.

¹⁰W. Hager, S. J. Linz, and P. Hänggi, *Europhys. Lett.* **40**, 393 (1997).

¹¹P. A. Thompson and G. S. Grest, *Phys. Rev. Lett.* **67**, 1751 (1991); T. Pöschel, *J. Phys. II* **3**, 27 (1993).

¹²H. M. Jaeger, C.-H. Liu, S. R. Nagel, and T. A. Witten, *Europhys. Lett.* **11**, 619 (1990).

¹³V. G. Benza, F. Nori, and O. Pla, *Phys. Rev. E* **48**, 4095 (1993).